ISBN: 978-3-95450-227-1 ISSN: 2673-5490 doi:10.18429/JACoW-IPAC2022-WEPOST021

THEORETICAL STUDY OF LASER ENERGY ABSORPTION TOWARDS ENERGETIC PROTON AND ELECTRON SOURCES

I. M. Vladisavlevici*[1,2], D. Vizman[2], E. d'Humières[1]
[1]University of Bordeaux – CNRS – CEA, CELIA, Talence, France
[2]West University of Timisoara, Faculty of Physics, Timisoara, Romania

Abstract

Our main goal is to describe and model the energy transfer from laser to particles, in the transparent regime of laser-plasma interaction in the ultra-high intensity regime, and using the results obtained to optimize laser ion acceleration. We investigate the case of an ultra high intensity (10^{22} W/cm^2) ultra short (20 fs) laser pulse interacting with a near-critical density plasma made of electrons and protons of density 5 n$_c$ (where $n_c = 1.1 \cdot 10^{21}$cm^{-3} is the critical density for a laser wavelength of $\lambda = 1\,\mu$m). Through 2D particle-in-cell (PIC) simulations, we study the optimal target thickness for the maximum conversion efficiency of the laser energy to particles. Theoretical modelling of the predominant laser-plasma interaction mechanisms predicts the particle energy and conversion efficiency optimization. Our studies led to an optimization of the target thickness for maximizing electron and proton acceleration.

INTRODUCTION

At the interaction of an ultra-high intensity laser pulse ($I \geq 10^{18}$ W/cm^2) with a plasma, the laser energy is transferred to the plasma constituents which are accelerated up to relativistic velocities for electrons. This energy transfer depends on the initial target and laser parameters [1–3], as well as on the interaction regime [4]. The absorption of laser energy determines the characteristics of the accelerated particles. There are multiple optimization models for maximizing the absorption of energy and the particles energies, depending on the interaction regime [5–8].

In this paper we analyse the case of an ultra-high intensity ultra-short laser pulse interacting with a near critical density target. We want to optimize the transfer of the laser energy to the particles and using the results obtained, to maximize the energy of the accelerated particles. In the first section is described the 2D particle-in-cell (PIC) simulation setup. In section 2 we report a dependence of the laser energy transfer on the target density. Section 3 presents the results on the optimization of the target thickness for maximizing electron and proton acceleration, which are in good agreement with the theoretical predictions. Finally, the main conclusions and perspectives are summarized in Section 4.

SIMULATION SETUP

The 2D PIC simulation setup consists of an ultra high intensity laser pulse interacting with a plasma (the target is considered fully ionized) as shown in Fig. 1. We consider a Gaussian laser profile, linearly polarized. The laser intensity is $I = 10^{22}$ W/cm^2 corresponding to a normalized field amplitude of $a_0 = 85$, where $a_0 = 0.85\sqrt{I_{W/cm^2}/10^{18} W/cm^2}\,\lambda_{\mu m}$. The laser wavelength is $\lambda = 1\,\mu$m and the laser transversal width is 25 µm. The pulse duration is 20 fs.

The plasma is made of electrons and protons and the initial proton and electron densities are equal $n_{i0} = n_{e0}$. The density has a uniform profile and the initial density is $n_{e0} = 5\,$n$_c$, where $n_c = 1.1 \cdot 10^{21}$cm^{-3} is the critical density for $\lambda = 1\,\mu$m. The target transversal width L_y is 30 µm and the target thickness L_x increases from 5 µm to 50 µm.

The simulation box size is 60 × 120 µm divided in 3840 × 7680 cells and the number of particles in each cell is 30 for each particle species. The simulations are performed with SMILEI [9] on the Curta machine of MCIA computing facility [10].

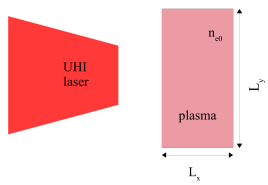

Figure 1: 2D PIC simulation setup: an ultra high intensity laser pulse irradiating a fully ionized target.

RESULTS ON ENERGY ABSORPTION

Fig. 2 shows the temporal evolution of the total energy in the simulations box. The initial electromagnetic laser energy is transferred to the plasma and is converted into 3 coefficients: A - the absorption coefficient representing the sum of the total kinetic energy of the particles and the radiation emitted by the electrons (see inset in Fig. 2) divided by the initial laser energy; R - the reflection coefficient representing the energy of the part of the laser which is reflected by the plasma and T - the transmission coefficient representing the energy of the part of the laser which passes through the target, both divided by the initial laser energy. The emission of radiation by electrons is simulated by two models: the continuous Landau-Lifshitz model ε_{rad} for low energy photons and a stochastic Monte Carlo model for the high energy photons [11].

Our goal is to maximize the absorption coefficient, by minimizing the other coefficients.

* iuliana.vladisavlevici94@e-uvt.ro

ISBN: 978-3-95450-227-1 ISSN: 2673-5490 doi:10.18429/JACoW-IPAC2022-WEPOST021

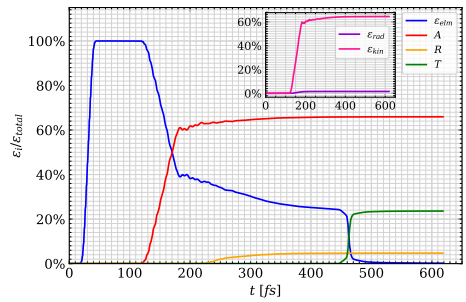

Figure 2: Time evolution of the total energy in the simulation box: ε_{elm} - the electromagnetic energy; ε_{kin} - the total kinetic energy of the particles; ε_{rad} - the energy radiated by electrons; A - the absorption coefficient; R - the reflection coefficient; T - the transmission coefficient. The target parameters are: the density $n_{e0} = 5\,\mathrm{n_c}$ and the thickness $L_x = 10\,\mu\mathrm{m}$. The laser parameters are: the normalized field amplitude $a_0 = 85$, the pulse duration $\tau_L = 20\,\mathrm{fs}$ FWHM and the focal spot size $w_0 = 12.5\,\mu\mathrm{m}$ FWHM.

The variation of the absorption coefficient with the target thickness is illustrated in Fig. 3. The absorption coefficient is increasing gradually with the target thickness until it reaches a plateau. After reaching the plateau, additional plasma will not significantly change the absorption coefficient. For the initial target density of $5\,\mathrm{n_c}$, the plateau is reached at a target thickness of $20\,\mu\mathrm{m}$, where 89% of the laser energy was converted in kinetic energy of the particles. By increasing the target thickness we successfully minimized the transmission coefficient to $T \leq 2\%$. However, a part of the laser pulse is reflected by the target, and the reflection coefficient depends on the target density. Consequently, we will define the optimum thickness L_0 for the laser energy absorption, as the thickness for which the absorption coefficient A does not change with more than 2%.

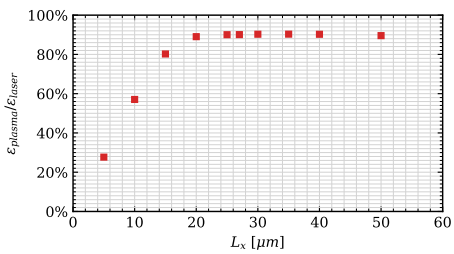

Figure 3: The absorption coefficient vs target thickness from 2D PIC simulations for $n_{e0} = 5\,\mathrm{n_c}$, $a_0 = 85$, $\tau_L = 20\,\mathrm{fs}$ FWHM and $w_0 = 12.5\,\mu\mathrm{m}$ FWHM.

RESULTS ON PARTICLE ACCELERATION

Electron Sources

At the interaction between the laser pulse and the target, the hot electrons predominantly absorb laser energy due to their high charge-to-mass ratio. They travel through the target and eventually reach the rear side of it. The protons, having a much lower charge-to-mass ratio move behind. This charge displacement gives rise to a strong quasi-electrostatic charge-separation field at the rear side of the target which in turn, accelerates the rear located protons and reinject the not very energetic electrons back inside the target, forming a return current. For a target thickness of $10\,\mu\mathrm{m}$, the maximum value of this quasi-electrostatic field in the 2D PIC simulation is 128 TV/m. The ultra relativistic electrons escape the electrostatic potential and propagate in the vacuum behind the target.

We obtained a broad energy spectrum for electrons, as shown in Fig. 4. The low energy electrons population represents the electrons which recirculate inside the target, and the high energy electrons population represents the electrons which escape the target at the rear side. The average energy of the electrons with the energy higher than 5 MeV is 17 MeV and the cutoff energy is 840 MeV.

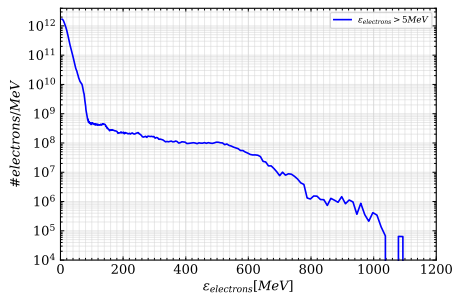

Figure 4: Electron energy spectrum from a 2D PIC simulation at 408 fs for $n_{e0} = 5\,\mathrm{n_c}$, $L_x = 10\,\mu\mathrm{m}$, $a_0 = 85$, $\tau_L = 20\,\mathrm{fs}$ FWHM and $w_0 = 12.5\,\mu\mathrm{m}$ FWHM.

The maximum electron energy after traveling through the simulation box was measured. The variation of it with the target thickness is shown in Fig. 5. The electron energy is maximized for low thicknesses, where the laser pulse is not fully absorbed and passes through the target. After reaching the maximum absorption, the maximum electron energy is stabilized in all cases at a value around 500 MeV.

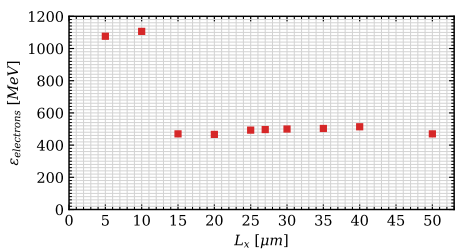

Figure 5: Maximum electron energy vs target thickness from 2D PIC simulations for $n_{e0} = 5\,\mathrm{n_c}$, $a_0 = 85$, $\tau_L = 20\,\mathrm{fs}$ FWHM and $w_0 = 12.5\,\mu\mathrm{m}$ FWHM.

Proton Sources

To study the proton acceleration mechanisms we consider that the target is made of two species of protons, front and

ISBN: 978-3-95450-227-1 ISSN: 2673-5490 doi:10.18429/JACoW-IPAC2022-WEPOST021

rear protons, named after their position in the target structure as shown in the inset of Fig. 6. The laser pulse comes from the left side and initially irradiates the front side of the target. For a high laser intensity and an overdense target, the laser pressure pushes masses of electrons, creating a strong electric field which accelerates the front located ions in the forward direction, a process known as Radiation Pressure Acceleration (RPA) [12]. In addition, as explained in the previous section, at the rear side of the target is created a strong quasi-electrostatic field which accelerates the rear located protons in the forward direction, a process known as Target Normal Sheath Acceleration (TNSA) [13, 14]. The RPA-accelerated protons can reach the rear side of the target where they are re-accelerated by the TNSA quasi-electrostatic field. In the simulations performed, the most energetic protons were originating from the rear side of the target as can also be seen in the protons phase-space from Fig. 6. The TNSA quasi-electrostatic field appears also in the front side of the target due to plasma expansion, accelerating backwards the front located protons.

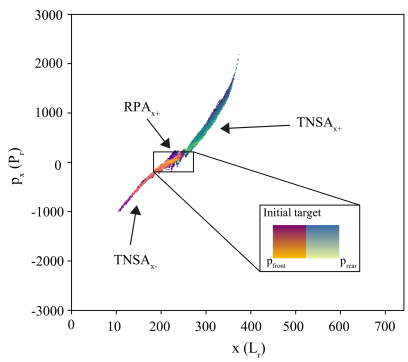

Figure 6: Proton phase space from a 2D PIC simulation for $n_{e0} = 5\,n_c$, $L_x = 10\,\mu m$, $a_0 = 85$, $\tau_L = 20\,fs$ FWHM and $w_0 = 12.5\,\mu m$ FWHM. The inset describes the initial repartition of protons inside the target. The main proton acceleration mechanisms are RPA and TNSA.

The variation of the maximum proton energy with the target thickness is shown in Fig. 7. The maximum proton energy is optimum for a 10 µm target thickness, which is very close to the Brantov theoretical prediction $l_{opt} = 0.5 a_0 \lambda n_c / n_{e0}$ [15]. At this thickness, 57% of the laser energy was converted in particle kinetic energy. For higher target thicknesses, the maximum proton energy decreases strongly. This is due to the spread of the hot electrons over a larger volume in the target, which results in a lower density of hot electrons, and in turn a lower quasi-electrostatic field and a lower energy for the accelerated protons.

The theoretical prediction for the maximum proton energy for a plasma expansion-like mechanism is given by [16]:

$$\varepsilon_{max,TNSA} = 2T_{hot} \ln^2 \{t_p + \sqrt{t_p^2 + 1}\} \quad (1)$$

where T_{hot} is the average energy of the hot electrons and t_p is the normalized acceleration time which is computed using

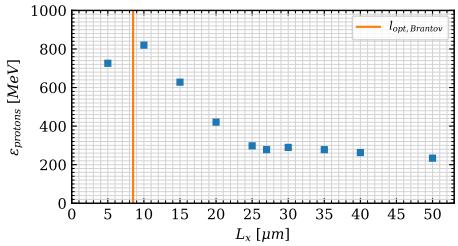

Figure 7: Maximum proton energy vs target thickness from 2D PIC simulations for $n_{e0} = 5\,n_c$, $a_0 = 85$, $\tau_L = 20\,fs$ FWHM and $w_0 = 12.5\,\mu m$ FWHM.

the total heated plasma volume, as found in the simulations. The expected maximum proton energy is 800 MeV which is in good agreement with the simulation value of 820 MeV.

CONCLUSIONS AND PERSPECTIVES

We studied the transfer of energy of an ultra high intensity ultra short laser pulse to a near critical density target. We aimed to maximize the absorption of energy, by minimizing the transmission and reflection coefficients. The optimum thickness to maximize the absorption of energy was 20 µm for an initial target density of 5 n_c, which corresponds to an absorption coefficient of 89%. We found a dependence of the absorption coefficient on the target density, which should be further investigated. Next steps could also include the study of the variation of the absorption coefficient with the laser parameters. Our studies lead to the optimization of the target thickness for maximizing particles energies. The main particles characteristics are summarized in Table 1 assuming that the 2D simulation results are valid over the laser transverse dimension in the z-direction to calculate the charge.

Table 1: Particle Beam Characteristics for 5 n_c, $L_x = 10\,\mu m$, $a_0 = 85$, $\tau_L = 20\,fs$ FWHM and $w_0 = 12.5\,\mu m$ FWHM

Particle	Maximum energy	Total energy >300 MeV	Total charge >300 MeV
Electron	1.1 GeV	2.37 J	5.2 nC
Proton	820 MeV	19.5 J	47 nC

ACKNOWLEDGEMENTS

Computer time for this study was provided by the computing facilities MCIA (Mésocentre de Calcul Intensif Aquitain) of the Université de Bordeaux and of the Université de Pau et des Pays de l'Adour.

This work was supported by Romanian National Authority for Scientific Research PN 75/2018, Agence Nationale de la Recherche project ANR-17-CE30-0026-Pinnacle, WUT - JINR collaboration project 05-6-1119-2014/2023 (2/2019; 86/2020; 103/2021) and Erasmus+ Student grant (2018/2019; 2019/2020; 2020/2021).

ISBN: 978-3-95450-227-1 ISSN: 2673-5490 doi:10.18429/JACoW-IPAC2022-WEPOST021

REFERENCES

[1] K.G. Estabrook, E.J. Valeo, and W.L. Kruer, "Two-dimensional relativistic simulations of resonance absorption", *The Physics of Fluids*, vol. 18, no. 9, p. 1151, 1975. doi:10.1063/1.861276

[2] F. Brunel, "Not-So-Resonant, Resonant Absorption", *Physical Review Letters*, vol. 59, no. 1, p. 52, 1987. doi:10.1103/PhysRevLett.59.52

[3] W.L. Kruer and K. Estabrook, "**J**×**B** heating by very intense laser light", *The Physics of Fluids*, vol. 28, no. 1, p. 430, 1985. doi:10.1063/1.865171

[4] E. Lefebvre and G. Bonnaud, "Transparency/Opacity of a Solid Target Illuminated by an Ultrahigh-Intensity Laser Pulse", *Physical Review Letters*, vol. 74, no. 11, p. 2002, 1995. doi:10.1103/PhysRevLett.74.2002

[5] J. Denavit, "Absorption of High-Intensity Subpicosecond Lasers on Solid Density Targets", *Physical Review Letters*, vol. 69, no. 21, p. 3052-3055, 1992. doi:10.1103/PhysRevLett.69.3052

[6] A. Debayle *et al.*, "Electron heating by intense short-pulse lasers propagating through near-critical plasmas", *New Journal of Physics*, vol. 19, no. 123013, 2017. doi:10.1063/1.1333697

[7] R. Mishra *et al.*, "Model for ultraintense laser-plasma interaction at normal incidence", *New Journal of Physics*, vol. 20, no. 043047, 2018. doi:110.1088/1367-2630/aab8db

[8] A. Pazzaglia *et al.*, "A theoretical model of laser-driven ion acceleration from near-critical double-layer targets", *Communications Physics*, vol. 3, no. 133, 2020. doi:10.1038/s42005-020-00400-7

[9] J. Derouillat *et al.*, "SMILEI : A collaborative, open-source, multi-purpose particle-in-cell code for plasma simulation", *Computer Physics Communications*, vol. 222, p. 351-373, 2018. doi:10.1016/j.cpc.2017.09.024

[10] University of Bordeaux, Mesocentre de Calcul Intensif Aquitaine - Curta machine, https://redmine.mcia.fr/projects/cluster-curta

[11] M. Lobet *et al.*, "Modeling of radiative and quantum electrodynamics effects in PIC simulations of ultra-relativistic laser-plasma interaction", *Journal of Physics: Conference Series*, vol. 688, no. 012058, 2016. doi:10.1088/1742-6596/688/1/012058

[12] A.P.L. Robinson *et al.*, "Radiation pressure acceleration of thin foils with circularly polarized laser pulses", *New Journal of Physics*, vol. 10, no. 013021, 2008. doi:10.1088/1367-2630/10/1/013021

[13] R.A. Snavely *et al.*, "Intense High-Energy Proton Beams from Petawatt-Laser Irradiation of Solids", *Physical Review Letter*, vol. 85, no. 2945, 2000. doi:10.1103/PhysRevLett.85.2945

[14] S.C. Wilks *et al.*, "Energetic proton generation in ultra-intense laser–solid interactions", *Physics of Plasma*, vol. 8, no. 542, 2001. doi:10.1063/1.1333697

[15] A.V. Brantov *et al.*, "Ion energy scaling under optimum conditions of laser plasma acceleration", *Physical Review Special Topics - Accelerators and Beams*, vol. 18, no. 021301, 2015. doi:10.1103/PhysRevSTAB.18.021301

[16] J. Fuchs *et al.*, "Comparative spectra and efficiencies of ions laser-accelerated forward from the front and rear surfaces of thin solid foils", *Physics of Plasmas*, vol. 14, no. 053105, 2007. doi:10.1063/1.2720373